Computers and Concrete, *Vol. 19, No. 6 (2017) 641-649*
DOI: https://doi.org/10.12989/cac.2017.19.6.641

Modeling of the ITZ zone in concrete: Experiment and numerical simulation

Yanuar Setiawan[1a], Buntara S. Gan[*2] and Ay Lie Han[3b]

[1]Department of Civil Engineering, Faculty of Civil Engineering and Planning, Islamic University of Indonesia, Jalan Kaliurang Km. 14.5, Sleman, Yogyakarta, 55584, Indonesia
[2] Department of Architecture, College of Engineering, Nihon University, 1 Nakagawara, Tokusada, Koriyama, Fukushima, 963-8642, Japan
[3]Department of Civil Engineering, Faculty of Engineering, Diponegoro University, Jalan Prof. H. Soedarto S.H., Tembalang, Semarang, 50275, Indonesia

(Received August 27, 2015, Revised February 11, 2017, Accepted February 13, 2017)

Abstract. The discovery of the Interfacial Transition Zone (ITZ) by Farran in 1956 initiated a new era in the study of the behaviour of concrete. Acknowledged as the weak link, this ITZ was studied extensively, numerically as well as experimentally. While the complementary experimental tests illustrated the visual behaviour of this specimen under increasing monotonic compression loading, a perfect bond within the ITZ has also been studied by using finite element analysis for comparison purposes. Finite element analysis was used to evaluate the degree of correctness and precision of the proposed ITZ model. This paper discusses the use of the cutoff bar in finite element modeling, representing the ITZ of a single aggregate (inclusion) in a mortar matrix. Experiments were conducted to investigate the influence of the ITZ model on the single inclusion specimen's strength. The model was tested for some inclusions that varied in dimension and shape. The effect of inclusion shape on the stress concentrations of the specimens was examined. The aim of this research work is to propose a simple yet accurate ITZ model to be used in the commercially available finite element software packages.

Keywords: FEM; cutoff bar; ITZ; compressive strength; full bond

1. Introduction

The discovery of the Interfacial Transition Zone (ITZ) by Farran (1956) initiated a new era in the study of the aggregate (inclusion) behaviour in concrete. Fig. 1 shows the stress distribution around the aggregate in the mortar under compression, which was introduced by Vile (1968). The ITZ is found to be a zone where the bond between the inclusion and mortar is broken due to the combination of tension and shear. The thickness of the ITZ between the inclusion and mortar in concrete is between 20 and 50 m. This minuscule dimension leads to difficulties in describing its exact behaviour under increasing load. Several experimental studies have found that the thickness of the ITZ corresponds to the mean radius of cement grains (Escadeillas and Maso 1991). The thickness and properties of the ITZ could also depend on the aggregate's size (Elsharief *et al*. 2003) and mineralogical composition (Tasong *et al*. 1999).

Many experimental techniques have been developed to characterize the microscopic features of the ITZ (Prokopski and Halbiniak 2000, Sorelli *et al.* 2008, Wang *et al*. 2009). Original experimental techniques on the load-displacement behaviour in tension and shear of the ITZ were conducted (Han and Sabdono 2011, Han and Nuroji 2010), and their results were implemented in a finite element model (FEM). The discrepancies observed in FEM results in comparison with experimental measurements on the mechanical behaviour of concrete are often explained by the fact that the ITZ is not taken into account in the model. Codes and specifications of concrete do not take into account the ITZ in the calculations because they are empirical, and the ITZ effects are not considered to be of a magnitude relevant to engineering applications.

In a previous study, the ITZ was represented by a linkage element consisting of two springs (Han *et al*. 2012). The substantiation of this FEM by the experimental data underlined that the load-displacement behaviour as predicted by the FEM was correct. Although this linkage element model gave satisfactory results, its use was limited to cylindrical inclusions since the algorithms were developed based on an ITZ angle smaller than 180o inwards with respect to the aggregate.

Some attempts have been introduced to consider the modelling of the ITZ by numerical models (Bentz and Garboczi 1999, Garboczi *et al*. 2000, Garboczi and Berryman 2001, Lee and Park 2008) and analytical models (Neubauer *et al*. 1996, Garboczi 1997, Nadeau 2003, Zheng *et al.* 2012) to simulate the effective properties of concrete as a heterogeneous material. Some methods tried to incorporate the ITZ by using empirical formulas (Bourdette *et al.* 1995, Hashin and Monteiro 2002, Nadeau 2002, Ke *et al.* 2010). However, there was no association related to the effective behaviour of concrete.

Even though computing work has become cheap and

∗Corresponding author, Professor
E-mail: buntara@arch.ce.nihon-u.ac.jp
[a]M.Eng.
E-mail: yanuar.setiawan@uii.ac.id
[b]Associate Professor
E-mail: ayliehan@hccnet.nl

ISSN: 1598-8198 (Print), 1598-818X (Online)

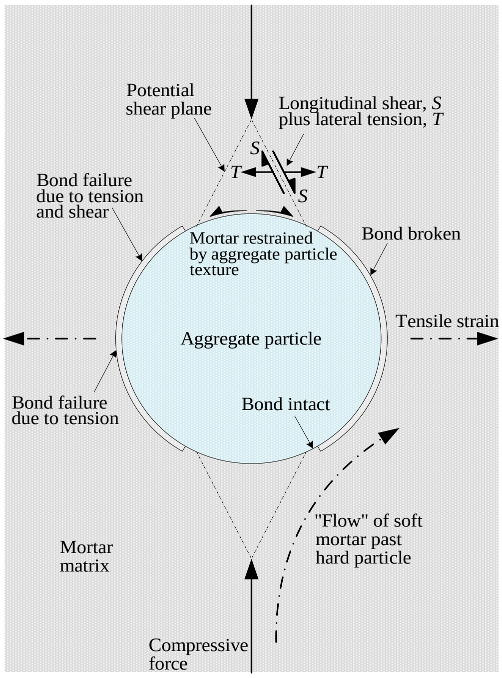

Fig. 1 The stress distribution around the inclusion under compression (Vile 1968)

processes have become faster, recent numerical models still prohibit the inclusion of the fine scale of the ITZ in the simulation. To overcome this weakness, the cutoff bar was proposed in combination with the use of available commercial nonlinear finite element software to study the behaviour of the ITZ. A range of cylindrical aggregate inclusions varying in diameter as well as triangular, diamond, and square shaped inclusions were prepared in the laboratory to serve as a validation tool for the FEM results. Additionally, the properties of the mortar matrix and the aggregate were tested based on the ASTM standards and serve as input to the FEM. As it was proven to be accurate, the FEM was able to run a theoretical full bond condition in the ITZ, and a comparison of the compressive strength behaviour between the actual ITZ and the fully bonded model was conducted.

2. Experimental programme and results

The laboratory-based experiments are distinguished by the tests performed to obtain the material properties, that is, the mortar, the aggregate, and the ITZ, and the specimens for the purposes of FEM validation.

2.1 Response of the ITZ and the behaviour of materials

The software required the mortar and aggregate mechanical properties, namely the cylindrical uniaxial compressive strength *f'c*, the Poisson's ratio *υ*, and the Young's modulus E. The mortar specimens cast to generate these data were 100×200 mm cylinders based on the ASTM C 39 Standard. The cylinders were kept moist and tested at the age of 28 days. The mortar in this study had a compressive strength *f'c* of 31 MPa, Poisson's ratio of 0.22, and Young's modulus of 31 GPa. The stress-strain relationship was formulated based on the FIB Model Code 2010. The aggregate specimens were cylinders sized 20.8×40 mm and were water-cooled diamond core drilled from the bulk aggregate. These aggregates were classified as diorite, consisting of the minerals plagioclase and pyroxene and having a porphyritic texture. The aggregate had a compressive strength of 159 MPa with a Poisson's ratio of 0.25 and a constant modulus of 75 GPa.

The load-displacement responses of the ITZ in tension and shear were tested independently, assuming an autonomous behaviour of the two responses, in the finite element analysis. The load-displacement response in tension was found to follow a quadratic function with an ultimate load per area of 109.9 N/mm^2 and a secant tangent modulus (kn) of 33.3 kN/mm/mm^2. The response in shear exhibited a contribution of bond and friction. The load at bond failure was measured as 423.3 N/mm^2, which was significantly higher than the capacity of the ITZ in tension. The initial tangent modulus (kt) was computed as 26.5 kN/mm/mm^2 (Han and Sabdono 2011, Han and Nuroji 2010). Fig. 2 shows the ITZ stiffness in the normal and tangential directions as the input for the FEM.

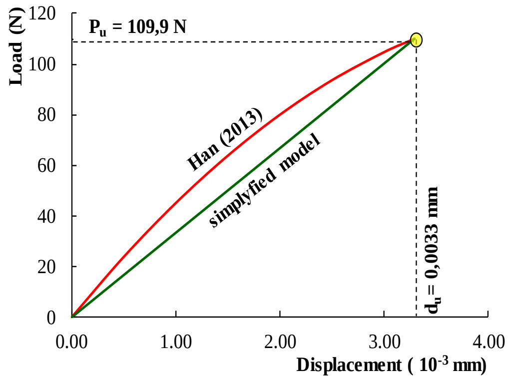

(a) Normal direction

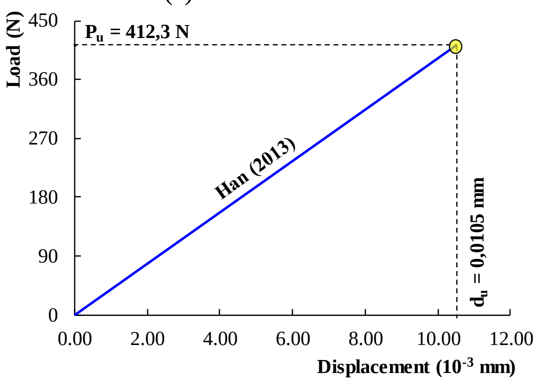

(b) Tangential direction

Fig. 2 ITZ stiffness model in the normal and tangential directions (Han 2013)

2.2 Validation of specimens

To enable evaluation of the proposed cutoff bar for modelling the ITZ and to examine its accuracy, identical laboratory specimens were produced with dimensions of

Table 1 Details of ITZ validation specimens

Specimen	Designation	Diameter (mm)
Cylindrical	BC0	20.85
Cylindrical	BC1	28.35
Cylindrical	BC2	45.56
Triangular	BTR	Center width: 30
Diamond	BD	Diagonal length: 28.35
Square	BSQ	Side length

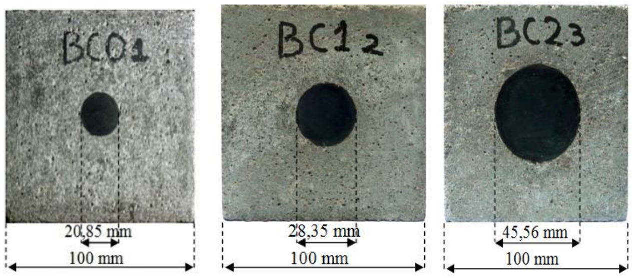

(a) Cylindrical specimens with varying diameters

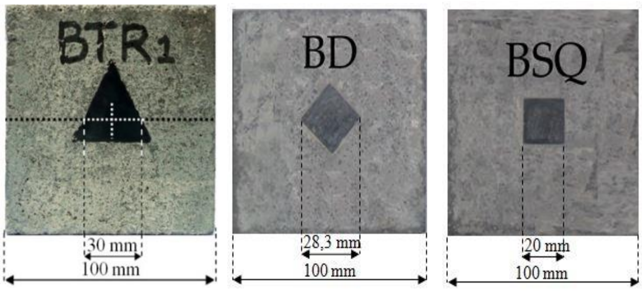

(b) Triangle (c) Diamond (d) Square

Fig. 3 Specimens with inclusion variation

100×100 mm with a thickness of 50 mm. This size was favoured since extensive research on inclusions has been conducted using this basic model (Akçaoğlu *et al.* 2004, Bremner and Holm 1986, Maher and Darwin 1977). The validation specimens had the same material properties and dimensions as the FEM. Four basic inclusion shapes were chosen: cylindrical, triangular, diamond, and square. The cylindrical inclusions had a range of diameters of 20.85, 28.35, and 45.56 mm. The triangular inclusion had a side length of 40 mm. The diamond (90°-oriented square) and square inclusions had equal side lengths of 20 mm (Fig. 3). For each type, eight specimens were prepared, from which six valid data were produced. The specifications of the specimens are shown in Table 1.

The specimens were cast, and the water-cement content was designed to a minimal by adding a superplasticizer to the mix. The specimens were kept moist by the submerging method and tested at the age of 28 days. The cast was made from Jati wood (Tectona grandis) and sealed at its seams, and waterproofing was conducted by applying a thin layer of grease at the inner surface of the cast. The aggregate inclusions were made the saturated surface dry, a condition were the surface of the aggregates are dry, but inter-particle voids are saturated with water, to minimize water absorption. This reducing the development of a water film surrounding the inclusion, which would intensify the

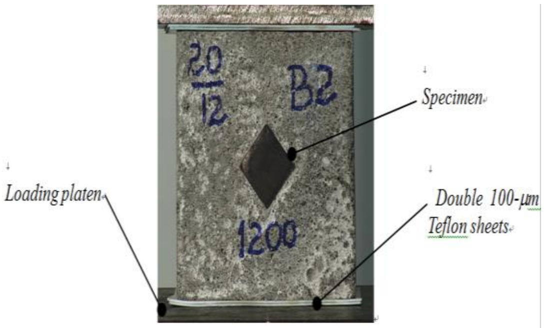

Fig. 4 Laboratory test setup

weakening of the ITZ bond. The vertical placement of inclusions assured a no-bleeding condition in the vicinity of the aggregates.

The specimens were dried and levelled to obtain a smooth and flat surface using a spirit/bubble lever. Prior to testing, a double 100-μm Teflon (polytetrafluoroethylene) sheet separated by a layer of bearing grease was placed on top and at the bottom of the specimen to minimize the confinement effects originating from the loading platen (RILEM 2000). The recorded load-displacement curves were corrected by the response of the Teflon layers. The load was applied with a constant increment of 1.800 N/s in accordance with the ASTM 109 standard. This load increment was also used in the FEM to ensure the same behaviour under increasing monotonic loading (Fig. 4).

3. Finite element analysis

3.1 Material behaviour and failure criteria

STRAND7 nonlinear software (2015) was used to incorporate the ITZ cutoff bar into the model. The model was constructed as a two-dimensional plane stress element. The load acts in-plane, and the only active degrees of freedom are the movements in this reference plane. All out-of-plane degrees of freedom were constrained using the boundary conditions in the global coordinate system. The mortar matrix was assumed to be isotropic, and the constitutive stress-strain relationship of the mortar matrix as expressed in the FIB Model Code for Concrete Structures 2010 was adopted.

In the STRAND7 software, the Max-Stress yield criteria are suitable for representing the nonlinear behaviour of the failure envelope of the mortar matrix. The envelope also defines a differentiation in principal stress combinations between biaxial tension, biaxial compression, and tension-compression.

The inclusion properties used in this study were assumed to be isotropic with a linear stress-strain behaviour following Hooke's law. The failure of the inclusion material never occurs since the compressive strength of the inclusion is substantially higher than that of the mortar.

3.2 The ITZ model

The linkage element for modelling the ITZ as developed

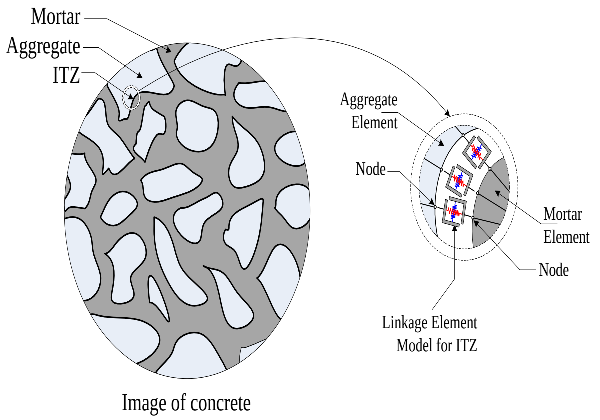

Fig. 5 Spring element modelling for the ITZ

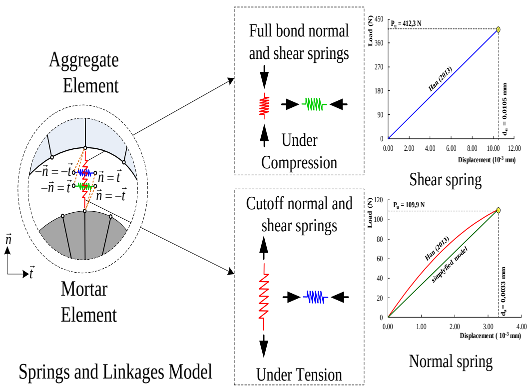

Fig. 6 Cutoff bar element for modelling the ITZ

by Han *et al.* (2012) consists of a double spring element. This linkage element has been used extensively for modelling the bond between reinforcing steel and concrete (Ngo and Scordelis 1967, Nilson 1968, Scordelis *et al.* 1974) and in modelling the concrete fracture mechanism (Jagota and Bennison 1994). The results prove a very close and accurate approximation to real bond behaviour. In meshing, the double node technique was accessed, and two nodes having the same coordinates were assigned within the ITZ. One node was placed in the aggregate and the other in the mortar matrix. The two nodes were connected by the two springs. The spring perpendicular to the ITZ surface represented the normal response of the ITZ while the parallel spring corresponded to the shear behaviour. The springs had zero thickness and were therefore considered appropriate to represent the minuscule ITZ (Fig. 5). This model was further adjusted to enable its accommodation in the nonlinear software.

The basic principles of the linkage element's dual movement were adopted for the beam element used in this study. The beam element chosen was the cutoff bar. The cutoff bar element is programmed based on the ultimate load in tension and compression. As soon as the force within the axial component of the cutoff bar exceeds this ultimate load, the ITZ is assumed to have failed. The cutoff bar element can be designed as a tensile or a compression response bar or a combination of both. The bar in this study had a thickness of 1.0 mm. Ongoing studies reflected that a thickness of 0.2 mm is manageable by the program. Attempts to import meshing data produced by a mesh generator are being conducted at the moment and will allow a zero thickness for the cutoff bar.

The cutoff bar consisted of three basic elements, one perpendicular to the ITZ surface and defined as being the normal response, and two parallel to the ITZ surface, representing the shear modes (Fig. 6). In modelling the shear stiffness by using horizontal springs, both nodes at the interface is connected to a positive and a negative direction of linkages. The linkages will act in opposite directions to each other to model the compression and tension conditions due to the movement of both adjacent nodes at the interface. The failure criterion of the ITZ was defined at ultimate load (Fig. 2). As for the mode of shear, the first part of the bilinear curve was used to describe the behaviour in the direction tangential to the ITZ, since the point of inflection demarcates the loss of the bond in the ITZ.

The general cutoff bar model only accommodates normal responses; therefore the model was modified to enable the response in the shear direction within the ITZ. The technique applied in this study is to superimpose two cutoff bars, one to account for the tension-shear response and the other to characterize the compression-shear mode. Further, a link was introduced to disseminate the shear displacement between the inclusion and mortar node to the cutoff bar. The final step was to restrain the cutoff bar in the direction perpendicular to the ITZ.

When an increment load was applied to the FEM, the relative displacement in the direction perpendicular to the ITZ was calculated. Two conditions were considered: compression and tension. Under compression, a full bond in the ITZ was assumed. In the modelling, a large substantial value of the normal stiffness modulus was used for the cutoff bar.

In the case of tension, two failure modes were distinguished. The first was the case in which the tensile force in the ITZ exceeded the ultimate load, resulting in a bond loss in the direction of normal tension. However, since the shear capacity is much higher than the normal capacity, the stiffness modulus in shear still contributed to the stiffness of the cutoff bar, and ITZ failure was due to tension. The second was the case in which the shear force surpassed the ultimate shear load. Upon losing the bond in shear, the tension stiffness simultaneously dropped to zero, and, in this case, the ITZ failed in shear.

4. Test results and FEM validation

A prototype FEM model, as shown in Fig. 7, was used for validation purposes. The material properties of the mortar, the aggregate, and the ITZ were superimposed on the program. The failure criteria for the ITZ in both shear and tension were set based on the experimental data. The loading increment was adjusted to the rate of laboratory testing. To simulate the behaviour of the laboratory specimens, a uniform strain on the top and bottom of the model was created by adjusting the bottom constraints and applying a uniform load, creating a uniform displacement of the top nodes.

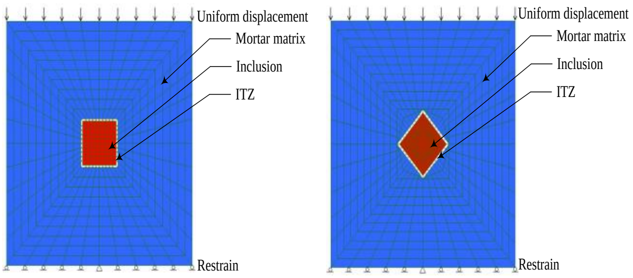

Fig. 7 Finite element model for analysing the ITZ

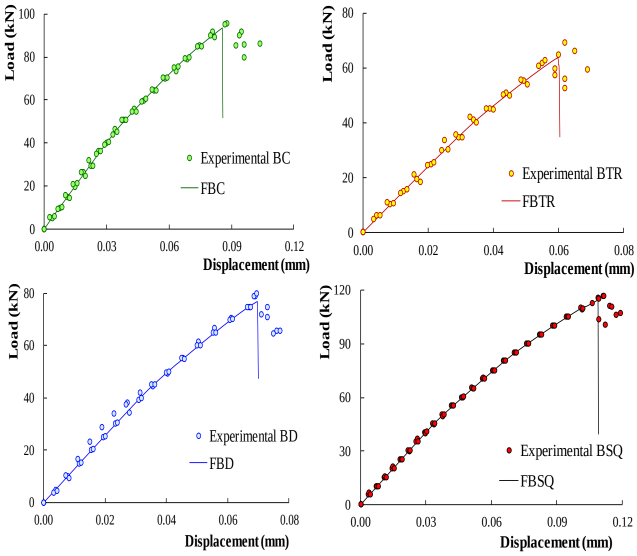

Fig. 8 Load-displacement responses of FEM and experiments

Table 2 Details of FEM simulation models

Specimen	Designation	Dimensions (mm)	FEM Model
Cylindrical	BC0	Diameter:20.85	–
Cylindrical	BC1	Diameter:28.35	FC
Cylindrical	BC2	Diameter:45.56	–
Triangular	BTR	Center width:30	FTR
Diamond	BD	Diagonal length:28.35	FD
Square	BSQ	Side length:20	FSQ

During the loading stages, the direct iteration technique was performed to obtain convergence between the external and internal forces, and the load and displacement data at convergent points were recorded. The FEM was run for all four models shown in Table 2, and the resulting load-displacement responses were plotted against the experimentally obtained data as can be seen in Fig. 8.

Fig. 8, the lines show the load-displacement response as predicted by the FEM, while the points represent the experimentally recorded data. It was shown that the stiffness behaviour predicted by the model was in good agreement with the actual load-displacement response, and the experimental data were situated in the vicinity of the FEM predicted curve. The cutoff bar model proved to be excellent for inclusions with a straight side as was the case for the triangle, thus overcoming the weakness of the

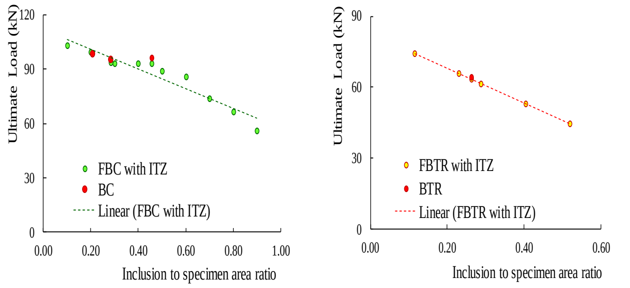

(a) FBC model and BC specimen (b) FBTR model and BTR specimen

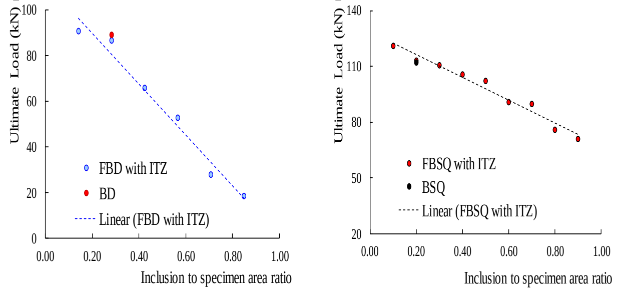

(c) FBD model and BD specimen (d) FBSQ model and BSQ specimen

Fig. 9 Ultimate load and inclusion-to-specimen area ratio relationships

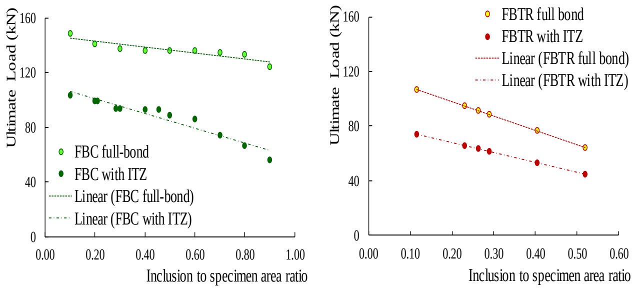

(a) BC specimens (b) BTR specimens

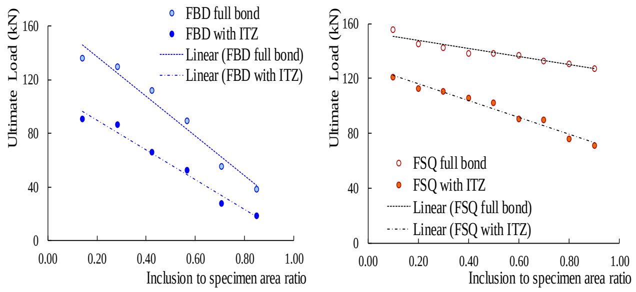

(c) BD specimens (d) BSQ specimens

Fig. 10 Full bond versus ITZ ultimate loads

previously developed double linkage element in Han and Sabdono (2011). After reaching the ultimate load, the program recorded a sudden stiffness drop. The experimental results, however, demonstrated post-peak behaviour and strain softening.

5. The FEM as an instrument of analysis

Having been proven to be reliable, the FEM was further

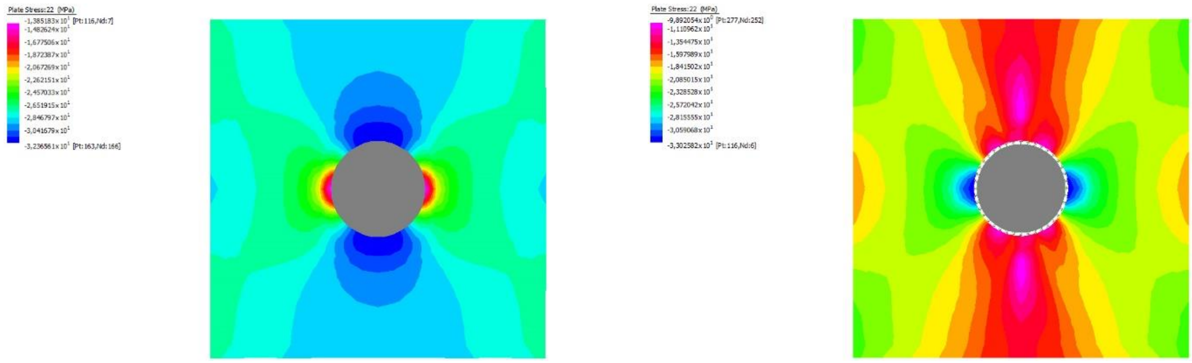

(a) FC model (comparison between fully bonded and with ITZ)

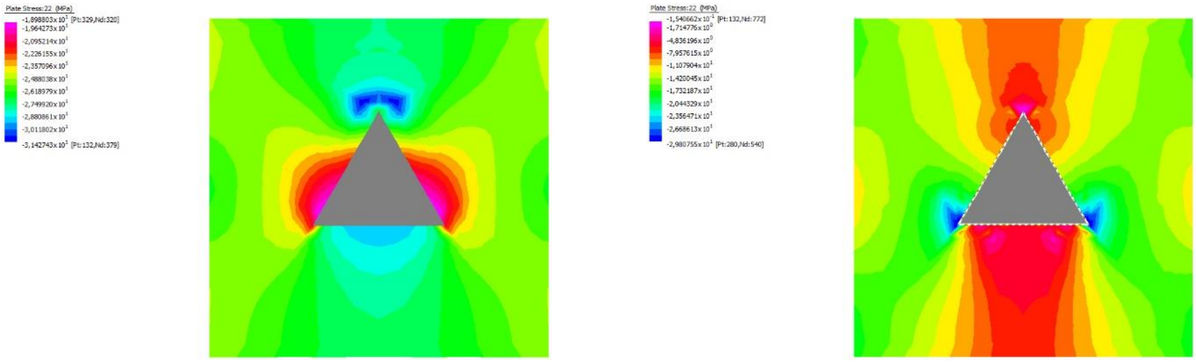

(b) FTR model (comparison between fully bonded and with ITZ)

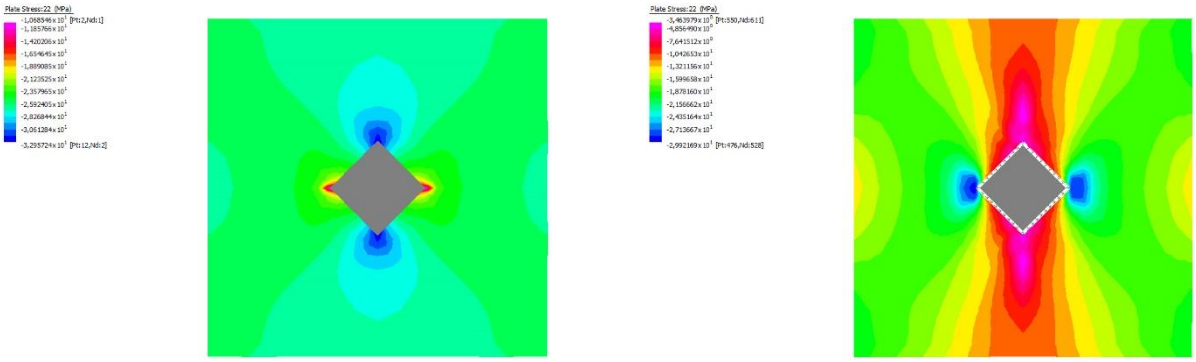

(c) FD model (comparison between fully bonded and with ITZ)

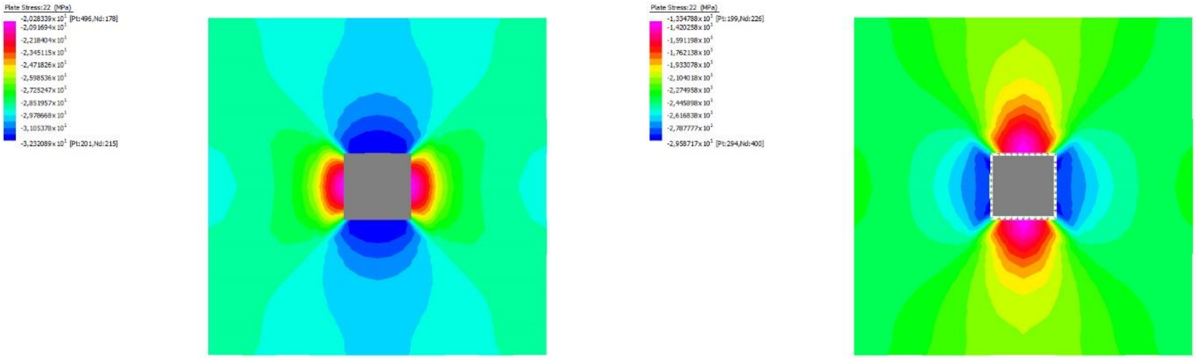

(c) FSQ model (comparison between fully bonded and with ITZ)

Fig. 11 Comparison of the principal stress $\sigma 22$ contours of the fully bonded model and the model with ITZ

utilized to analyse the response of the compressive strength as a function of the increase in inclusion diameter. As can be seen from the four models FC, FTR, FD and FSQ, a relatively higher inclusion-to-specimen area ratio resulted in a decrease in compressive strength. To study this phenomenon, a set of inclusion diameters with an inclusion-to-specimen area ratio ranging from 0.1 to 0.9 was run through the program and the ultimate load was recorded.

The functionality of the ITZ was further investigated. A full bond between the aggregate inclusion and the mortar matrix was simulated. The four representative inclusion models were evaluated for this purpose.

5.1 On the aspect ratio of the inclusion diameter

To evaluate the response of the inclusion-to-specimen area ratio perpendicular to the line of loading, the FEM was run for a range of the inclusion shapes, and the predicted ultimate load was recorded (Fig. 9). The results are compared with the experimental ones.

The path of this load response as a function of the increase in the inclusion-to-specimen area ratio suggested that the larger the inclusion-to-specimen area ratio, the lower the ultimate load-carrying capacity of the specimen. The response followed an almost linear path, which was confirmed by the test results of the experimental specimens BC1, BTR, BD, and BSQ. There were good agreements between the actual load and simulation results at which the specimen failed. Hence the data strengthen the conclusion that there is a reduction in capacity of the specimens.

This declining ultimate load response is possibly influenced by two factors: the large disparity between the properties of the aggregate and mortar and the presence of the ITZ. The inclusions have a much higher stiffness modulus when compared to the mortar matrix. Also, the constitutive stress-strain response under increasing compression load is linear up to failure. The mortar matrix has a highly nonlinear response, even at very low stress levels. These factors will lead to high-stress concentrations in the mortar matrix strip adjacent to the inclusions. Since this mortar strip decreases as a function of inclusion diameter increase, the stresses in the vicinity of the aggregate are significantly enhanced, leading to premature cracking in the tension area of the mortar strip. Further, larger inclusions will have larger ITZ areas. As the ITZ is the weak link in the concrete, large ITZ areas will have a more pronounced negative influence on the load-carrying capacity of the specimen. These findings were confirmed by the research work of Suarjana *et al.* (1998). In that study, multiple steel aggregates were used and the number of inclusions was increased gradually, thus increasing the ITZ area. To study the ITZ phenomenon, the FEM was run for an idealized full-bond ITZ

5.2 The full theoretical bond in the ITZ

In the laboratory, creating a specimen with a perfectly fully bonded ITZ is not an easy task. However, with the help of the developed FEM, the hypothetical load-carrying capacity of a full-bond ITZ can be evaluated. Fig. 10 shows the comparison between a full bond and the actual behaviour of the ITZ for the same range of inclusion-to-specimen area ratios. Fig. 11 shows the contours of the second principal stresses of both the full bond and the ITZ calculated by FEM.

As can be seen, the full-bond models resulted in a much higher ultimate load-carrying capacity when compared to the ITZ models. The degradation of compressive strength reached 50 to 44% for inclusion-to-specimen area ratios smaller than 0.5 but was predicted to reach 60 to 120% for the larger ratios. The negative ITZ effect thus becomes pronounced when the ITZ ratio is higher. However, this behaviour is also influenced by the high stress concentrations in the mortar.

In Fig. 11, the distributions of the principal stress $\sigma22$ for both the full-bond model and the model with an ITZ show different contour distributions. The principal $\sigma22$ was chosen to represent the stress concentration at the ITZ because it is the direction perpendicular to the main loading direction that is prone to fracture due to tension. By implementing the ITZ model in the analyses, the differences in stress concentration patterns are clearly observed. However, the full-bond model gives smaller stress concentration zones and hence underestimates the ultimate load of the specimens. From these results, it is clear that the implementation of the ITZ model is necessary to accurately predict the ultimate load capacity of concrete with inclusions such as steel reinforcement, aggregates, and others. Study on the multi-inclusion behaviour were conducted (Han *et al.* 2015a, b) and largely strengthened the outcome of this study.

6. Conclusions

The validation procedure demonstrated that the cutoff bar representing the behaviour of the ITZ between aggregates and the mortar matrix in concrete was versatile. The FEM predicted the exact stiffness development of a single inclusion aggregate to a high degree of accuracy. The model, however, slightly overestimated the ultimate load at which the specimen failed. The source of this weakness lies in the meshing techniques; finer meshing is required in areas with high stress concentration to avoid premature failure of large elements. This problem could be overcome by running a trial analysis, diagnosing the areas with high stress concentrations, and introducing finer meshing in these regions. The constant load increment that was used in extracting the load-displacement response is also a factor that has to be taken into consideration. When the specimen stiffness decreases, a gradually declining load increment will lead to a better prediction of the ultimate load. The cutoff bar model could be further utilized to analyse the behaviour of any variation of ITZs, provided that the individual tension and shear behaviour were available.

The FEM that was run for varying inclusion-diameter ratios showed that the ultimate strength of the specimen decreased as a function of increases in the inclusion-to-specimen area ratio. The curve followed a linear path. This behaviour can be explained as a collective negative effect between the increase of the ITZ area and the stress concentration enhancement in the mortar adjacent to the inclusion. These stress concentrations are a contribution of the stiffness disparity between the aggregate and mortar, the nonlinear behaviour of the mortar matrix, and reduction of the mortar strip.

The theoretical full-bond condition showed that on average a 45 to 120% increase in compressive strength is gained when a good bond is assured in the ITZ, suggesting that smaller aggregates, however the condition of the ITZ, are more advantageous as compared to the larger inclusions. Whiles some standards advise the use of sharp-edged aggregates, the study of triangular inclusions suggested that the sharper the inclusion angle, the lower the load levels at which cracking first occurs and the lower the ultimate load of the specimens. More data on angled inclusions can be found in papers published on this topic (Han *et al*. 2014a, b, Han *et al*. 2015a, b, Han *et al*. 2017).

The proposal presented in this work is easy to implement and is recommended for use in modelling the ITZ in concrete by using a commercial finite element software package. The present work presented a preliminary research on single inclusions in concrete. In future work, a multi-inclusions model, probabilistic- and stochastic-based methods for incorporating the inclusions in concrete, and a proposal for practical FEM will be studied. The model can further be expanded to study the effect of additives such as silica fume to the fracture behaviour of aggregate inclusions in concrete.

References

Akçaoğlu, T., Tokyay, M. and Çelik, T. (2004), "Effect of coarse aggregate size and matrix quality on ITZ and failure behavior of concrete under uniaxial compression", *Cement Concrete Compos*., **26**(6), 633-638.

Bentz, D. and Garboczi, E. (1999), "Computer modelling of interfacial transition zone: Microstructure and properties", *Eng. Transp. Propert. Interf. Transit. Zone Cement. Compos*., **5**, 349-385.

Bourdette, B., Ringot, E. and Olivier, J.P. (1995), "Modelling of the transition zone porosity", *Cement Concrete Res*., **25**(4), 741-751.

Bremner, T.W. and Holm, T.A. (1986), "Elastic compatibility and the behavior of concrete", *ACI J. Proc*., **83**(2), 244-250.

Elsharief, A., Cohen, M. and Olek, J. (2003), "Influence of aggregate size, water cement ratio and age on the microstructure of the interfacial transition zone", *Cement Concrete Res*., **33**(11), 1837-1849.

Escadeillas, G. and Maso, J. (1991), "Approach of the initial state in cement paste, mortar and concrete", *Adv. Cement Mater*., 169-184.

Farran, J. (1956), "Contribution mineralogique a l'etude de l'adherence entre les constituants hydrates des ciments et les materiaux enrobes", *Rev. Mater. Constr*., **490-491**, 155-172.

Garboczi, E. (1997), "Stress, displacement, and expansive cracking around a single spherical aggregate under different expansive conditions", *Cement Concrete Res*., **27**(4), 495-500.

Garboczi, E. and Berryman, J. (2001), "New effective medium theory for the linear elastic moduli of a material containing composite inclusions", *Mech. Mater*., **33**(8), 455-470.

Garboczi, E., Bentz, D., Shane, J., Mason, T. and Jennings, H. (2000), "Effect of the interfacial transition zone on the conductivity of Portland cement mortars", *J. Am. Ceram. Soc*., **83**(5), 1137-1144.

Han, A.L, Gan, B.S., Yuniarto, R., Yesica, A. and Editia, R.N. (2015), "Inclusion-to-specimen volume ratio influence on the strength and stiffness behaviors of concrete: An experimental study", *Appl. Mech. Mater*., **845**, 113-118.

Han, A.L. (2013), "Modeling the stiffness properties of the aggregate-to-mortar interfacial transition zone in concrete", Ph.D. Dissertation, Diponegoro University, Semarang, Indonesia.

Han, A.L. and Nuroji. (2010), "The normal and shear modulus properties of the interfacial transition zone in concrete: newly developed testing procedures", *Proceedings of the 35th Coral Anniversary Conference on Our World in Concrete and Structures, Challenge of the Low Carbon Age*, Singapore, August.

Han, A.L. and Sabdono, P. (2011), "Experimental study of the load-displacement response of the interfacial transition zone in concrete", *Proceedings of the 3rd International Conference on European Asian Civil Engineering Forum (EACEF-2011), Designing and Constructing Sustainability*, Yogyakarta, Indonesia, September.

Han, A.L., Gan, B.S. and Setiawan, Y. (2014a), "The influence of single inclusions to the crack initiation, propagation and compressive strength of mortar", *Proc. Eng*., **95**, 376-385.

Han, A.L., Gan, B.S. and Setiawan, Y. (2015), "The aggregate multi-inclusion interaction and interface influence on the compression behavior of concrete", *Implement. Innovat. Ideas Struct. Eng. Proj. Manage*., 695-700.

Han, A.L., Gan, B.S., Suryanto, B. and Priastiwi, Y.A. (2017), "Influence of the stiffness modulus and volume fraction of inclusions on compressive strength of concrete", *Proc. Eng*., **171**, 760-767.

Han, A.L., Nurhuda, I. and Setiawan, Y. (2014b), "The effect of aggregate shape and configuration to the concrete behavior", *Smart Sci*., **2**(2), 85-90.

Han, A.L., Sabdono, P. and Purnomo, J. (2012), "Finite element modeling of the transition zone between aggregate and mortar in concrete", *Proceedings of the 1st International Conference on Sustainable Civil Engineering Structures and Construction Materials (SCESCM)*, Yogyakarta, Indonesia, September.

Hashin, Z. and Monteiro, P. (2002), "An inverse method to determine the elastic properties of the interphase between the aggregate and the cement paste", *Cement Concrete Res*., **32**(8), 1291-1300.

Jagota, A. and Bennison, S.J. (1994), "Spring-network and finite element models for elasticity and fracture, in: Non-linearity and breakdown in soft condensed matters", *Proceedings of the Workshop in Calcutta*, Delaware, U.S.A., July.

Ke, Y., Ortola, A.L., Beaucour, S. and Dumontet, H. (2010), "Identification of microstructural characteristics in lightweight aggregate concretes by micromechanical modelling including the interfacial transition zone (ITZ)", *Cement Concrete Res*., **40**(11), 1590-1600.

Lee, K.M. and Park, J.H. (2008), "A numerical model for elastic modulus of concrete considering interfacial transition zone", *Cement Concrete Res*., **38**(3), 396-402.

Maher, A. and Darwin, D. (1977), "Microscopic finite element model of concrete", *Proceedings of the 1st International Conference on Mathematical Modeling III*, St. Louis, U.SA., August-September.

Nadeau, J. (2002), "Water-cement ratio gradients in mortar and corresponding effective elastic properties", *Cement Concrete Res*., **32**(3), 481-490.

Nadeau, J. (2003), "A multiscale model for effective moduli of concrete incorporating ITZ water-cement ratio gradients, aggregate size distributions, and entrapped voids", *Cement Concrete Res*., **33**(1), 103-113.

Neubauer, C., Jennings, H. and Garboczi, E. (1996), "A three-phase model of the elastic and shrinkage properties of mortar", *Adv. Cement-Bas. Mater*., **4**(1), 6-20.

Ngo, D. and Scordelis, A.C. (1967), "Finite element analysis of reinforced concrete beams", *ACI J. Proc*., **64**(3), 152-163.

Nilson, A.H. (1968), "Nonlinear analysis of reinforced concrete by the finite element method", *ACI J. Proc*., **65**(9), 757-766.

Prokopski, G. and Halbiniak, J. (2000), "Interfacial transition zone in cementitious materials", *Cement Concrete Res*., **30**(4), 579-583.

RILEM Technical Committee 148-SSC (2000), "Strain softening of concrete-test method for compressive softening", *Mater. Struct./Materiaux et Constr*., **33**, 347-351.

Scordelis, A.C., Ngo, D. and Franklin, H.A. (1974), "Finite element study of reinforced concrete beams with diagonal tension cracks", *ACI Spec. Publ*., **42**, 79-102.

Sorelli, L., Constantinides, G., Ulm, F.J. and Toutlemonde, F. (2008), "The nano-mechanical signature of ultra high performance concrete by statistical nanoindentation techniques", *Cement Concrete Res.*, **38**(12), 1447-1456.

STRAND7, Rel 2.4 (2015), *Reference Manual*, Strand7 Pty Limited.

Suarjana, M., Besari, M.S. and Abipramono R. (1998), "Two-dimensional concrete models using metal aggregates", *Proceedings of the RILEM 2nd International Conference on Interfacial Transition Zone in Cementitious Composites*, **31**, 67-74.

Tasong, W.A., Lynsdale, C.J. and Cripps, J.C. (1999), "Aggregate-cement paste interface. Part I. Influence of aggregate geochemistry", *Cement Concrete Res.*, **29**(7), 1019-1025.

Vile, G.W.D. (1968), "The strength of concrete under short term static biaxial stress", *Proceedings of the International Conference on Structure of Concrete*, 275-287.

Wang, X.H., Jacobsen, S., He, J.Y., Zhang, Z.L., Lee, S.F. and Lein, H.L. (2009), "Application of nanoindentation testing to study of the interfacial transition zone in steel fiber reinforced mortar", *Cement Concrete Res.*, **38**(8), 701-715.

Zheng, J., Zhou, Z. and Jin, X. (2012), "An n-layered spherical inclusion model for predicting the elastic moduli of concrete with inhomogeneous ITZ", *Cement Concrete Compos.*, **34**(5), 716-723.

CC